

# We are IntechOpen, the world's leading publisher of Open Access books Built by scientists, for scientists

6,900

Open access books available

186,000

International authors and editors

200M

Downloads

Our authors are among the

154

Countries delivered to

TOP 1%

most cited scientists

12.2%

Contributors from top 500 universities



WEB OF SCIENCE™

Selection of our books indexed in the Book Citation Index  
in Web of Science™ Core Collection (BKCI)

Interested in publishing with us?  
Contact [book.department@intechopen.com](mailto:book.department@intechopen.com)

Numbers displayed above are based on latest data collected.  
For more information visit [www.intechopen.com](http://www.intechopen.com)



# Practical Application of Simulation Technique for the Resonators Using Piezoelectric Ceramics

Jeong-Ho Cho, Yong-Hyun Lee, Myung-Pyo Chun and Byung-Ik Kim  
*Korea Institute of Ceramic Engineering & Technology  
Korea*

## 1. Introduction

In this couple of decades, applications of piezoelectrics to resonators, sensors and actuators have been dramatically accelerated, in addition to the discovery of new materials and devices. Some of the highlights include electrostrictive materials for positioners, ferroelectric single crystals with very high electromechanical couplings for medical transducers, thin/thick films for Micro-Electro-Mechanical Systems starting from a sophisticated chemical technology, and multilayer type actuators fabricated by cofiring technique. All will provide a remarkable industrial impact in the 21<sup>st</sup> century.

Piezoelectric materials exhibit electromechanical coupling, which is useful for the design of devices for oscillating, sensing and actuation. The coupling is exhibited in the fact that piezoelectric materials produce an electrical displacement when a mechanical stress is applied and can produce mechanical strain under the application of an electric field. Due to the fact that the mechanical-to-electrical coupling was discovered first, this property is termed the direct effect, while the electrical-to-mechanical coupling is termed the converse piezoelectric effect.

The representative converse piezoelectric effect-applied example is a ceramic resonator. Frequency sources are a key component of much of today's electronics. Frequency sources are used as sensor, clocks and filters, and the ability to control the accuracy and stability of these devices is vital to their performance characteristics and ability to bring forth advancements in technology. Ceramic resonators stand between quartz crystals and LC/RC oscillators in regard to accuracy. They offer low cost and high reliability timing devices with improved start-up time to quartz crystals. The oscillation of ceramic resonators is dependent upon mechanical resonance associated with their piezoelectric crystal structure. The ceramic resonator oscillates in thickness-shear vibration mode for fundamental frequencies (typical less or equal than 8MHz) and thickness-longitudinal vibration mode for third-overtone mode (above 8MHz to 50MHz). Ceramic resonators have superior resonant impedance than quartz crystal, which offer much better start-up time. They have low cost because of high mass production rate, small size, no need for adjustment.

Recently, narrow frequency tolerance characteristics of piezoelectric ceramic resonators have been required for fabricating highly accurate electronic devices. Because of this trend, a low electromechanical coupling coefficient and a high mechanical quality factor have been

required in piezoelectric materials. Widely used piezoelectric materials such as lead zirconate titanate (PZT) type materials have electromechanical coupling coefficient of over 30% for the fundamental thickness extensional and thickness shear vibration modes. The third harmonic thickness extensional vibration mode has also been used for resonator applications and their electromechanical coupling coefficients are low; however spurious vibration from the fundamental mode resonance is inevitable in this type of resonator. Spurious modes occurrence is one of the significant problems for various applications because those spurious vibrations worked as the cause of occurring the malfunction of devices. Therefore, it is an important issue to implement the configuration which spurious vibration doesn't affect the fundamental vibration as designing the resonator.

## 2. Basic Theory of Piezoelectricity

To simulate the piezoelectric properties, it is important to evaluate the material constants of piezoelectric ceramics exactly. The piezoelectric effect can be seen as a transfer of electrical to mechanical energy and vice-versa. It is observed in many crystalline materials. The direct piezoelectric effect consists of an electric polarization in a fixed direction when the piezoelectric crystal is deformed. The polarization is proportional to the deformation and causes an electric potential difference over the crystal. The inverse piezoelectric effect, on the other hand, constitutes the opposite of the direct effect. This means that an applied electric field induces a deformation of the crystal. The piezoelectric effects are written as the set of linear equations. The expressions for the piezoelectric effect can be combined into one matrix expression by writing the relationship between strain ( $S$ , m/m) and electric displacement ( $D$ , C/m<sup>2</sup>) as a function of applied stress ( $T$ , N/m<sup>2</sup>) and applied field ( $E$ , V/m):

$$\begin{Bmatrix} S \\ D \end{Bmatrix} = \begin{bmatrix} s & d \\ d & \epsilon \end{bmatrix} \begin{Bmatrix} T \\ E \end{Bmatrix} \quad (1)$$

Where  $s$  is the mechanical compliance (m<sup>2</sup>/N),  $d$  is the piezoelectric strain coefficient (C/N), and  $\epsilon$  is the dielectric permittivity (F/m).

It can be inverted to write the expressions with stress and field as the dependent variables and strain electric displacement as the independent variables.

$$\begin{Bmatrix} T \\ E \end{Bmatrix} = \frac{1}{s\epsilon - d^2} \begin{bmatrix} \epsilon & -d \\ -d & s \end{bmatrix} \begin{Bmatrix} S \\ D \end{Bmatrix} \quad (2)$$

It is possible to generalize this result to the case of an arbitrary volume of piezoelectric materials. Consider a cube of piezoelectric material, although there is no assumptions regarding the direction in which the electric field is applied or the directions in which the material is producing stress or strain. It is used as the common convention that the 3 direction is aligned along the poling axis of the material (Figure 1).

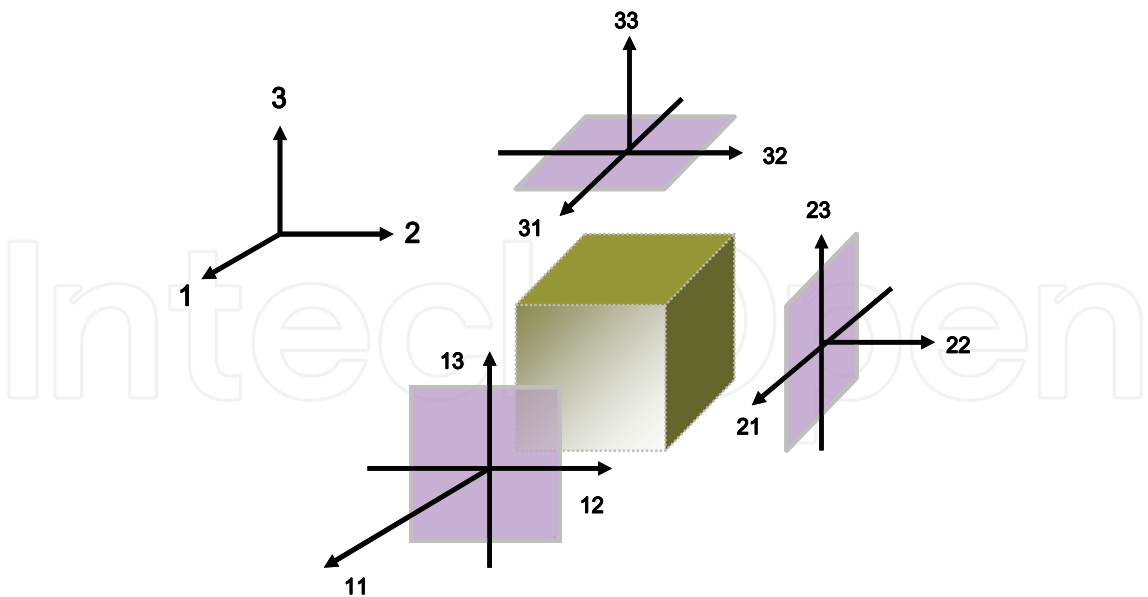


Figure 1. Piezoelectric cube indicating the coordinate axes of the 3D analysis

For a linear elastic material, the electric field and the electric displacement are expressed in terms of the vectors:

$$\mathbf{E} = \begin{pmatrix} E_1 \\ E_2 \\ E_3 \end{pmatrix} \tag{3}$$

$$\mathbf{D} = \begin{pmatrix} D_1 \\ D_2 \\ D_3 \end{pmatrix} \tag{4}$$

Similarly, the stress and the strain can be expressed in terms of the vectors. The components of stress and strain that are normal to the surface of the cube are donated  $T_{11}(T_1)$ ,  $T_{22}(T_2)$ ,  $T_{33}(T_3)$  and  $S_{11}(S_1)$ ,  $S_{22}(S_2)$ ,  $S_{33}(S_3)$ , respectively. There are six shear components,  $T_{12}(T_6)$ ,  $T_{13}(T_5)$ ,  $T_{23}(T_4)$ ,  $T_{21}(T_6)$ ,  $T_{32}(T_4)$ ,  $T_{31}(T_5)$  and  $S_{12}(S_6)$ ,  $S_{13}(S_5)$ ,  $S_{23}(S_4)$ ,  $S_{21}(S_6)$ ,  $S_{32}(S_4)$ ,  $S_{31}(S_5)$ . The parentheses are the compact notation for piezoelectric constitutive equations. With the compact notation form, the full constitutive relationships are represented by equations (5) and (6).

$$\begin{bmatrix} S_1 \\ S_2 \\ S_3 \\ S_4 \\ S_5 \\ S_6 \end{bmatrix} = \begin{bmatrix} s_{11} & s_{12} & s_{13} & s_{14} & s_{15} & s_{16} \\ s_{21} & s_{22} & s_{23} & s_{24} & s_{25} & s_{26} \\ s_{31} & s_{32} & s_{33} & s_{34} & s_{35} & s_{36} \\ s_{41} & s_{42} & s_{43} & s_{44} & s_{45} & s_{46} \\ s_{51} & s_{52} & s_{53} & s_{54} & s_{55} & s_{56} \\ s_{61} & s_{62} & s_{63} & s_{64} & s_{65} & s_{66} \end{bmatrix} \begin{bmatrix} T_1 \\ T_2 \\ T_3 \\ T_4 \\ T_5 \\ T_6 \end{bmatrix} + \begin{bmatrix} d_{11} & d_{12} & d_{13} \\ d_{21} & d_{22} & d_{23} \\ d_{31} & d_{32} & d_{33} \\ d_{41} & d_{42} & d_{43} \\ d_{51} & d_{52} & d_{53} \\ d_{61} & d_{62} & d_{63} \end{bmatrix} \begin{bmatrix} E_1 \\ E_2 \\ E_3 \end{bmatrix} \tag{5}$$

$$\begin{bmatrix} D_1 \\ D_2 \\ D_3 \end{bmatrix} = \begin{bmatrix} d_{11} & d_{12} & d_{13} & d_{14} & d_{15} & d_{16} \\ d_{21} & d_{22} & d_{23} & d_{24} & d_{25} & d_{26} \\ d_{31} & d_{32} & d_{33} & d_{34} & d_{35} & d_{36} \end{bmatrix} \begin{bmatrix} T_1 \\ T_2 \\ T_3 \\ T_4 \\ T_5 \\ T_6 \end{bmatrix} + \begin{bmatrix} \epsilon_{11} & \epsilon_{12} & \epsilon_{13} \\ \epsilon_{21} & \epsilon_{22} & \epsilon_{23} \\ \epsilon_{31} & \epsilon_{32} & \epsilon_{33} \end{bmatrix} \begin{bmatrix} E_1 \\ E_2 \\ E_3 \end{bmatrix} \quad (6)$$

As shown on equation (5) and (6), the elastic compliance matrix (s), the piezoelectric strain coefficient (d), and the dielectric permittivity ( $\epsilon$ ) have a different value depending on the crystal structure or symmetry of material. For example, in the equation (7), (8) and (9) it indicates respectively the elastic stiffness constant (c) to tetragonal, rhombohedral, and orthorhombic symmetry. The inverse matrix of the elastic compliance matrix (s) is the elastic stiffness constant (c).

$$\begin{bmatrix} c_{11} & c_{12} & c_{13} & 0 & 0 & 0 \\ c_{12} & c_{11} & c_{13} & 0 & 0 & 0 \\ c_{13} & c_{13} & c_{33} & 0 & 0 & 0 \\ 0 & 0 & 0 & c_{44} & 0 & 0 \\ 0 & 0 & 0 & 0 & c_{44} & 0 \\ 0 & 0 & 0 & 0 & 0 & c_{66} \end{bmatrix} \quad (7)$$

$$\begin{bmatrix} c_{11} & c_{12} & c_{13} & c_{14} & 0 & 0 \\ c_{12} & c_{11} & c_{13} & -c_{14} & 0 & 0 \\ c_{13} & c_{13} & c_{33} & 0 & 0 & 0 \\ c_{14} & -c_{14} & 0 & c_{44} & 0 & 0 \\ 0 & 0 & 0 & 0 & c_{44} & c_{14} \\ 0 & 0 & 0 & 0 & c_{14} & (c_{11} - c_{12}) / 2 \end{bmatrix} \quad (8)$$

$$\begin{bmatrix} c_{11} & c_{12} & c_{13} & 0 & 0 & 0 \\ c_{12} & c_{22} & c_{23} & 0 & 0 & 0 \\ c_{13} & c_{23} & c_{33} & 0 & 0 & 0 \\ 0 & 0 & 0 & c_{44} & 0 & 0 \\ 0 & 0 & 0 & 0 & c_{55} & 0 \\ 0 & 0 & 0 & 0 & 0 & c_{66} \end{bmatrix} \quad (9)$$

Most materials that has good piezoelectric properties in room temperature like BaTiO<sub>3</sub> and PbTiO<sub>3</sub> have a tetragonal symmetry of space group P4mm, however, Pb(Zr,Ti)O<sub>3</sub>-based

material mainly used in commercial products uses a morphotropic phase boundary composition where a tetragonal phase and a rhombohedral phase coexist. Another piezoelectric materials such as  $\text{NaNbO}_3$ ,  $\text{KNbO}_3$ ,  $\text{PbZrO}_3$ , and etc. show orthorhombic symmetry at room temperature. Therefore, to make an accurate simulation for devices using piezoelectric material, exact information on the space group of the crystal structure and the elastic stiffness constant or the elastic compliance constant is necessary.

### 3. Modelling

The resonant frequency of the ceramic resonator is directly influenced by the vibration mode in accordance with the configuration of ceramic. According to the trend of the recent electronic parts, the utilized-oscillation frequency of resonator is getting to a high frequency. The ceramic resonator which is mainly used in the MHz band mostly uses thickness shear vibration or thickness trapped vibration. Thickness shear vibration is used in the frequency range of 2 MHz ~ 8 MHz and the above frequency range uses thickness trapped vibration. The 2<sup>nd</sup> or 3<sup>rd</sup> overtone vibration is mostly used in the case of thickness trapped vibration rather than the 1<sup>st</sup> fundamental vibration. In the Fig. 2, it shows configuration, vibration direction and dipole array direction of the thickness shear vibration and thickness trapped vibration.

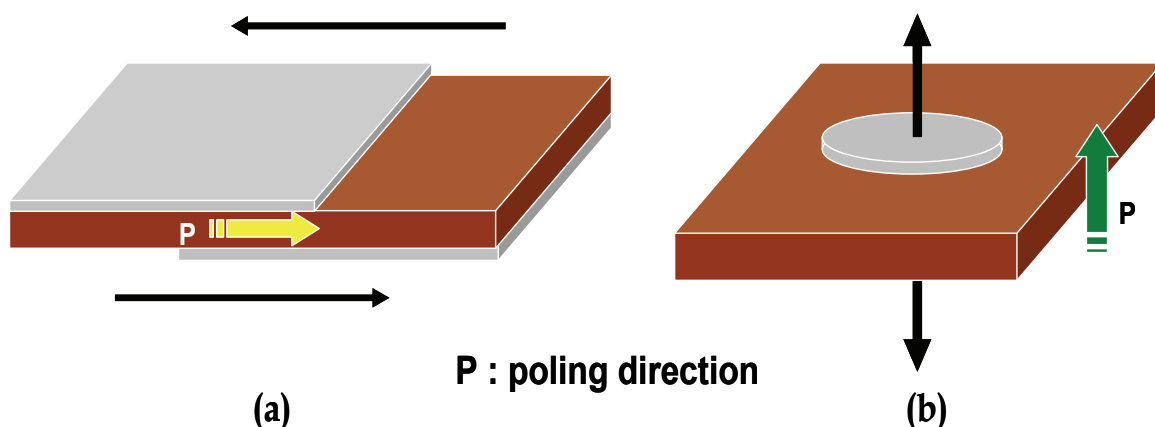


Figure 2. Configuration and vibration direction of thickness shear vibration and thickness trapped vibration (a) thickness shear mode; (b) thickness trapped mode

Commercial ceramic resonators over 8MHz have used mainly  $(\text{Pb},\text{La})\text{TiO}_3$ (PLT). However, manufacturers have been trying to apply layer structure compounds to resonator, these products are distributed to market recently.

The lattice of  $\text{PbTiO}_3$  exhibits a strong tetragonal distortion at 20°C. The lattice constant of a-axis ( $a$ ) increases smoothly as a result of heating, while the lattice of c-axis ( $c$ ) and  $c/a$  decrease. At 490-500°C the lattice constants  $c$  and  $a$  change sharply and the lattice becomes cubic.

PLT has a perovskite structure which the part of Pb is substituted by La and it shows a similar behavior to  $\text{PbTiO}_3$ . Layer-structure compounds such as  $\text{SrBi}_2\text{Nb}_2\text{O}_9$  are good alternatives to PLT. Its great anisotropy is one of the characteristics and over 60 kinds of compounds have been reported so far. Newnham et al. reported that the spontaneous polarization of layer structure compound is almost parallel in the plane of  $a$ ,  $b$  axis and located 2-dimensionally. Because these materials specifically have great anisotropy and their

poisson's ratio is less than 0.25, they show different characteristics of frequency dependence from the material based on  $\text{Pb}(\text{Zr,Ti})\text{O}_3$ . As explained above, PLT has tetragonal structure with  $P4mm$  of space group at room temperature. The layer structure compounds have  $Fmm2$  of orthorhombic symmetry at room temperature, although it has tetragonal symmetry of  $I4/mmm$  below a curie temperature. Therefore, the elastic stiffness constant matrix of equation 7 and 8 should be used respectively. However, because a very complicated process is needed to find all constants, layer structure compounds are also assumed as a tetragonal symmetry to simplify the simulation. In this case, the piezoelectric strain coefficient is formed like following equation.

$$d = \begin{bmatrix} 0 & 0 & 0 & 0 & d_{15} & 0 \\ 0 & 0 & 0 & d_{15} & 0 & 0 \\ d_{13} & d_{13} & d_{33} & 0 & 0 & 0 \end{bmatrix} \quad (10)$$

The elastic compliance constants and the piezoelectric strain coefficients can be found referring IEEE standard or Japan's EMAS. And in case of that EMAS was referred, they can be found by measuring electric properties with a material sample manufactured like shown in table 3. The configuration, dimension, and the representative constants of the standard material found here is shown in table 3.

Although several kinds of software can be used in a simulation of ceramic resonator, we used COMSOL Multiphysics. COMSOL Multiphysics is a good interactive environment for modeling and solving scientific and engineering problems based on partial differential equations. Thanks to the built-in physics modes it is possible to build models by defining the relevant physical quantities – such as material properties, loads, and constraints – rather than by defining the equations.

Fig. 3 is the comparison of the simulation result of disk shape sample with the actually measured result, using COMSOL Multiphysics. In Fig. 3, (a) represents the dimension of disk sample and (b) represents measured frequency dependence of impedance. (c) represents the impedance waveform by simulation. It conformed to the measured result even though there was little shift of resonant frequency.

## 4. Resonator and Vibration Mode

### 4.1 Thickness shear vibration (TS mode vibration)

The thickness shear vibration occurs when poling direction and voltage direction are perpendicular. This vibration mode is mostly used in 2 ~ 8 MHz band because it is less influenced by a spurious vibration when used as a resonator. Boundary condition is set to make displacement to be 0 on both sides of resonator. Poling is along the length direction, while voltage was supplied on both top and bottom sides setting poling direction and voltage direction perpendicular to make the thickness shear mode occur. The structure of resonator using thickness shear mode is shown in Fig. 4. It is 2 mm long and 0.15 mm thick.

Fig. 5 and 6 show general deformed shape in thickness shear mode and displacement distribution within the material in the same condition. In case of thickness shear vibration, most displacements are concentrated in the part where the electrode is present, and the maximum displacement occurs at the end of the electrode.

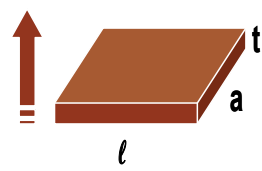
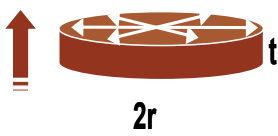
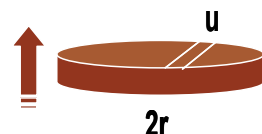
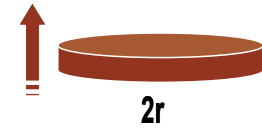
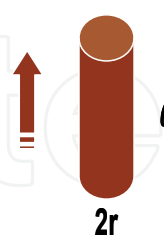

Vibrating mode		Dimension	Constant		Unit
lengthwise vibration		$a = 3\text{mm}$ $\ell = 12\text{mm}$ $t = 1\text{mm}$	$\epsilon_{33}^T$	155	-
			$s_{11}^E$	7.52	$10^{-12}$
radius vibration		$r = 7.5\text{mm}$ $t = 1\text{mm}$	$d_{31}$	-4.38	$10^{-12}$
		$r = 7.5\text{mm}$ $t = 0.5\text{mm}$ $u = 1\text{mm}$	$s_{12}^E$ $\sigma$	-1.51 0.201	$10^{-12}$ -
thickness vibration		$r = 5\text{mm}$ $t = 1\text{mm}$	$s_{13}^E$	-1.08	$10^{-12}$
longitudinal vibration		$r = 3\text{mm}$ $\ell = 15\text{mm}$	$s_{33}^E$	7.98	$10^{-12}$
			$d_{33}$	53	$10^{-12}$
thickness shear vibration		$a = 2.5\text{mm}$ $\ell = 10\text{mm}$ $t = 0.25\text{mm}$	$\epsilon_{11}^T$ $s_{44}^E$ $d_{15}$	220 16.3 55	- $10^{-12}$ $10^{-12}$

Table 1. Dimension of the sample recommended by EMAS and typical material properties of PLT



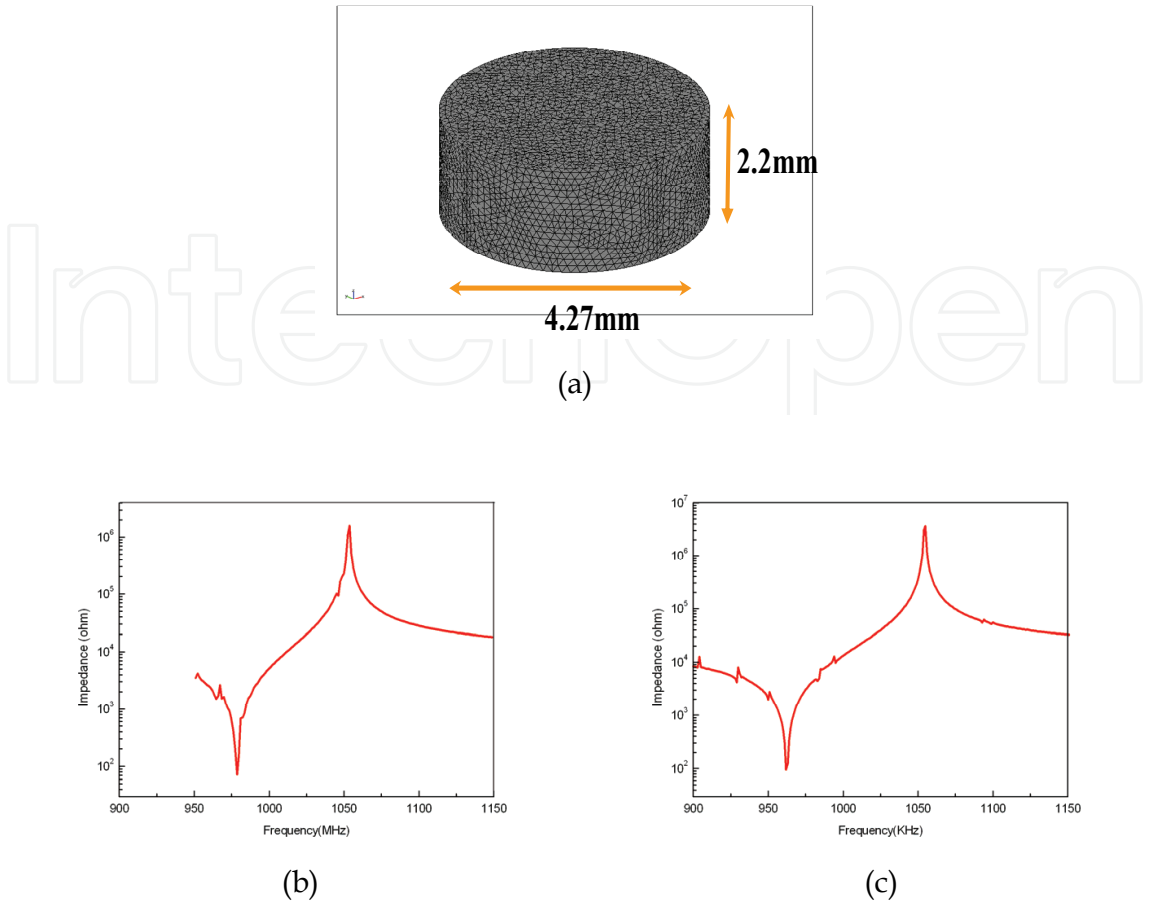


Figure 3. (a) Sample configuration; (b) Measured-impedance response; (c) Simulation result

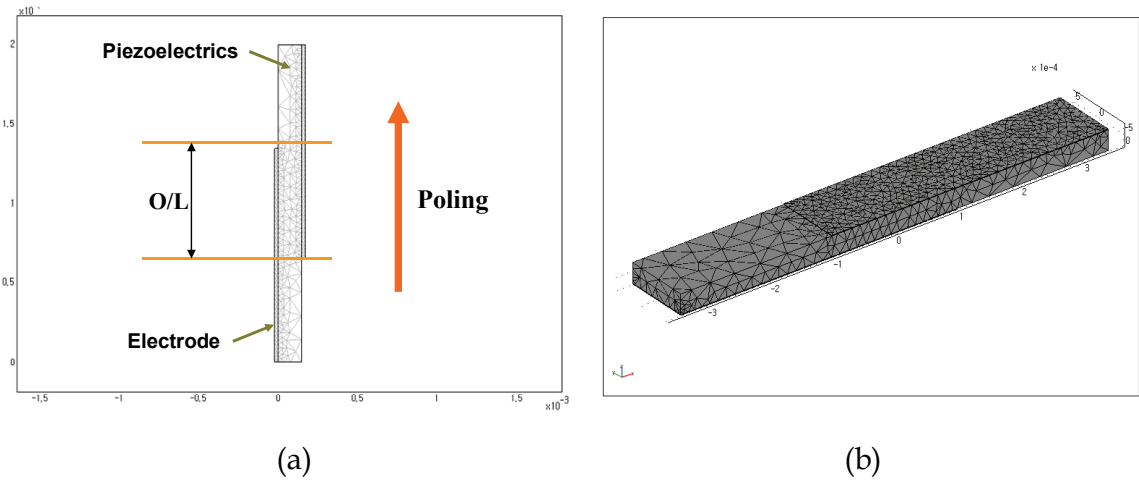
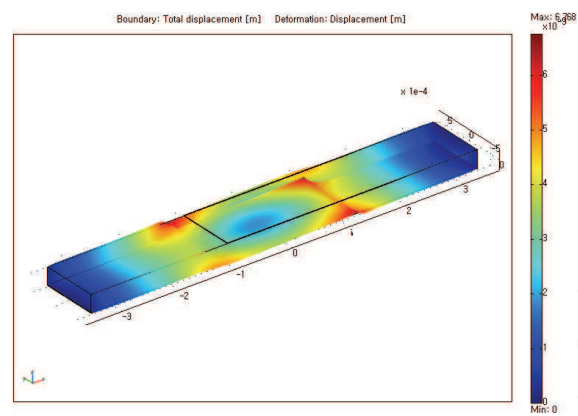
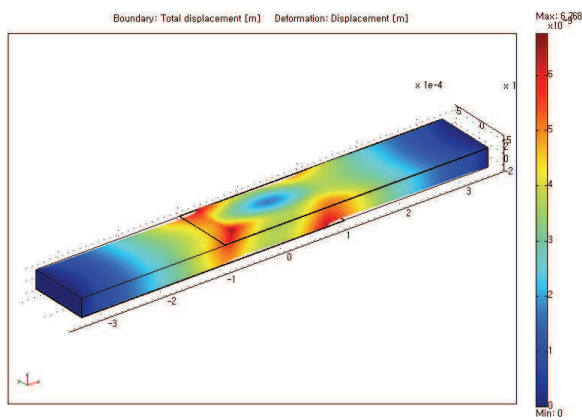


Figure 4. Simulation model for resonator using thickness shear vibration



(a)



(b)

Figure 5. Vibration configuration of thickness shear mode

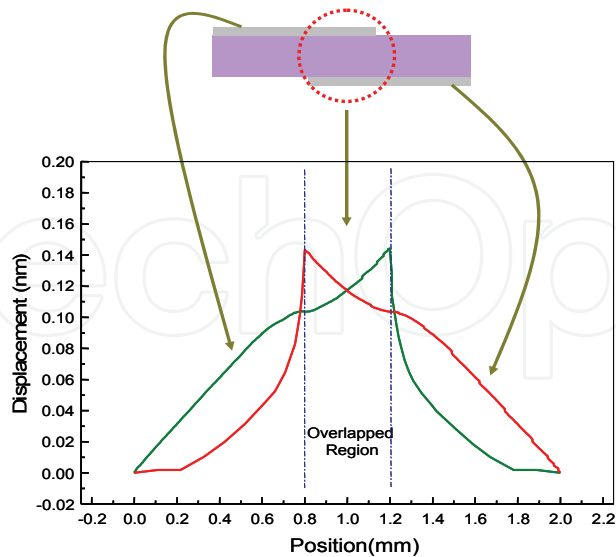


Figure 6. Displacement distribution in the thickness shear mode

The overlapped length (O/L) where top and bottom electrodes are overlapped has decisive effect on resonator property. Fig. 7 is showing frequency dependence of impedance according to the overlapping length (O/L). If O/L is small, the spurious vibration was is big

as the thickness shear vibration, and when O/L is not optimum, thickness shear vibration and other vibration is seen overlapped in the resonant frequency area.

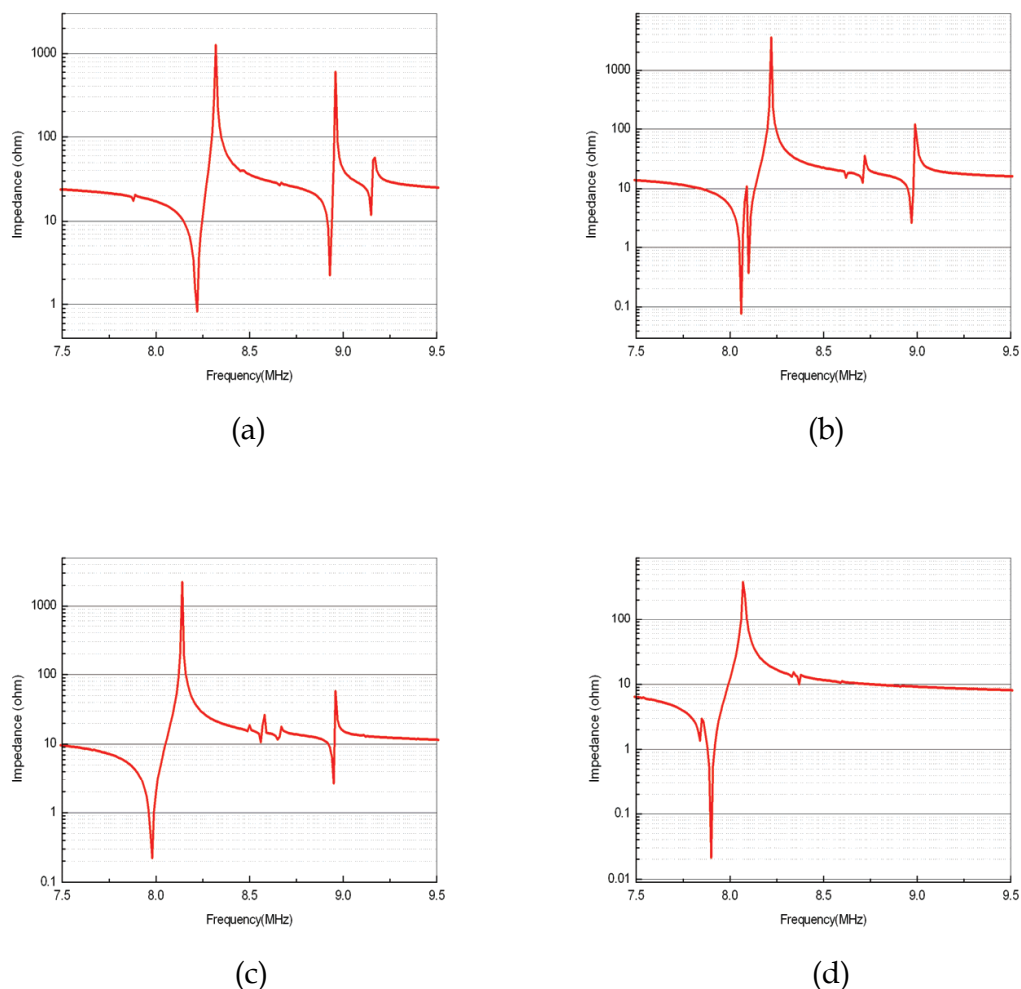


Figure 7. Frequency dependence of impedance (a) O/L = 0.2 mm; (b) O/L = 0.4 mm; (c) O/L = 0.6 mm; (d) O/L = 0.8 mm

#### 4.2.2 Thickness Extensional Vibration (TE2 mode vibration)

Recently the use of the TE2-mode vibration has been studied to minimize the resonator and elevate its functional features, in addition it was reported that the TE2-mode could promote the temperature feature and give a higher  $Q_m$ .

Fig. 8 shows the basic model for the simulation of TE2 mode and it is 1.5 mm wide, 0.5 mm long. The height was set based on 0.2 mm. Two sheets of ceramic were layered in TE2 resonator, the internal electrode is located between 2 sheets. Fixed point is set to make displacement 0 at the end of the resonator in length direction. Poling is in thickness direction. Round electrodes were attached to both top and bottom sides of resonator to supply the voltage here. Poling direction and voltage direction were set to be same in order to make the thickness extending mode occur. Generally, both sides of outside electrode are to be same pole, and the opposite pole is to be connected in the internal electrode to operate.

Fig. 8(c) shows poling direction and voltage direction. A vibration shape of TE2 mode occurring in this condition is shown in Fig. 9.

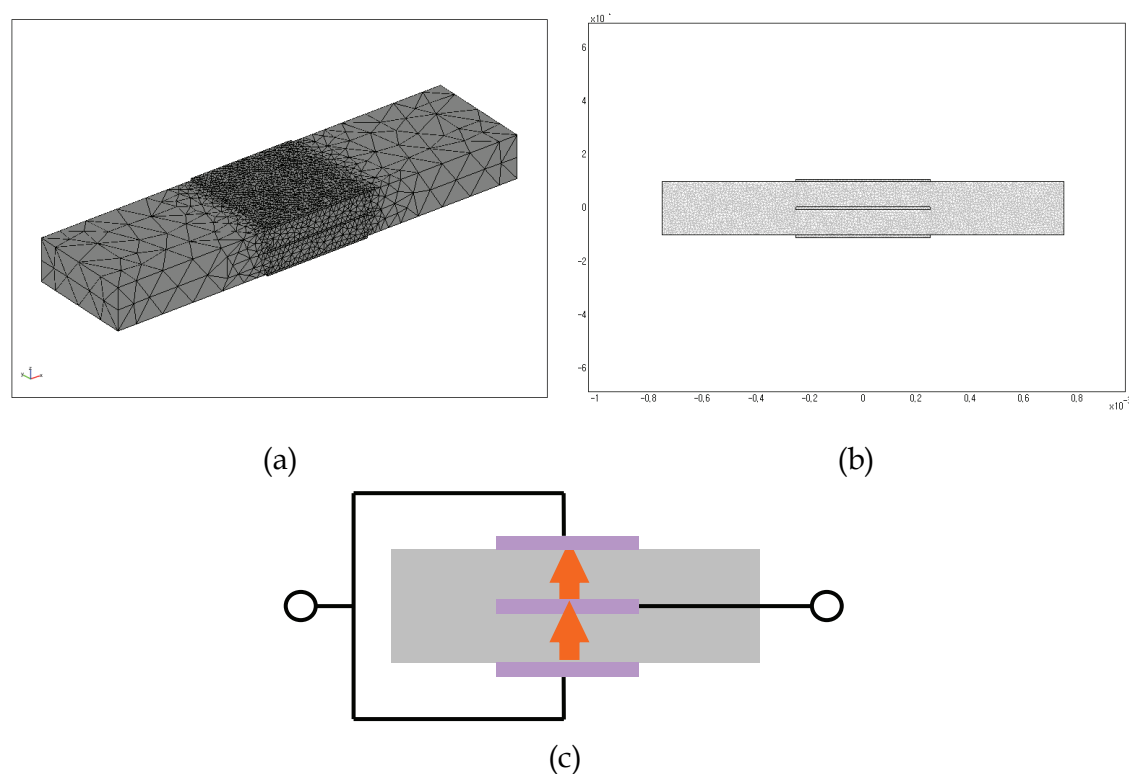


Figure 8. Simulation model for resonator using TE2 mode vibration

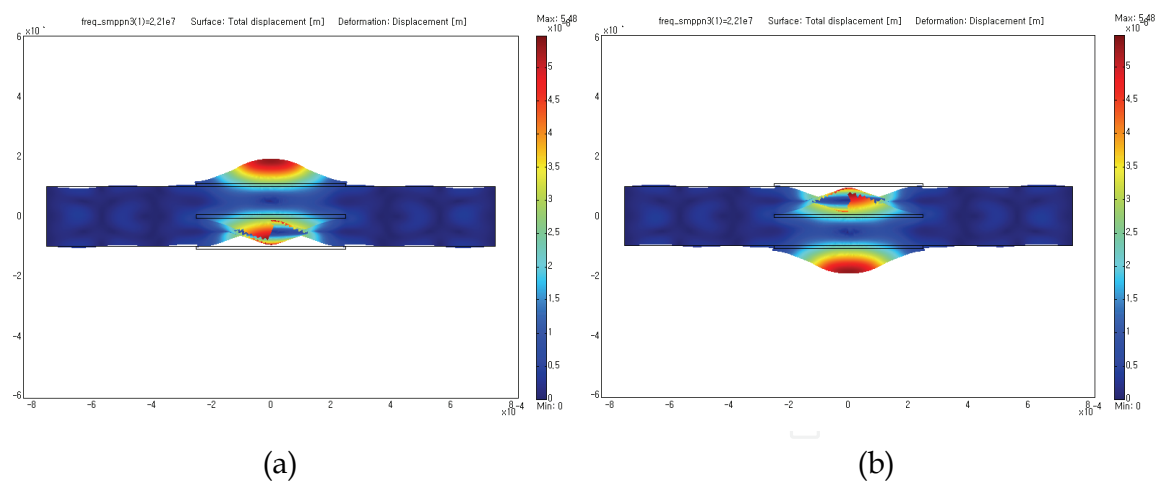


Figure 9. Vibration shape of TE2 mode vibration

In case of a resonator using TE2 mode, the electrode diameter has the most effect on impedance. The simulation result of the frequency dependence of displacement in piezoelectric ceramics with the electrode diameter is shown in Fig. 10. When electrode diameter becomes smaller, the amplitude of spurious vibration becomes very high to influence on TE2 mode vibration. On the other hand, when electrode diameter becomes larger, the resonant frequencies of TE2 mode vibration and a spurious vibration become closer. In case of that the electrode is 0.6 mm, it is expected that two vibrations become very

close to lead an interaction. Therefore, to keep main vibration out of the influence of spurious vibration, the optimum dimension of electrode should be formed.

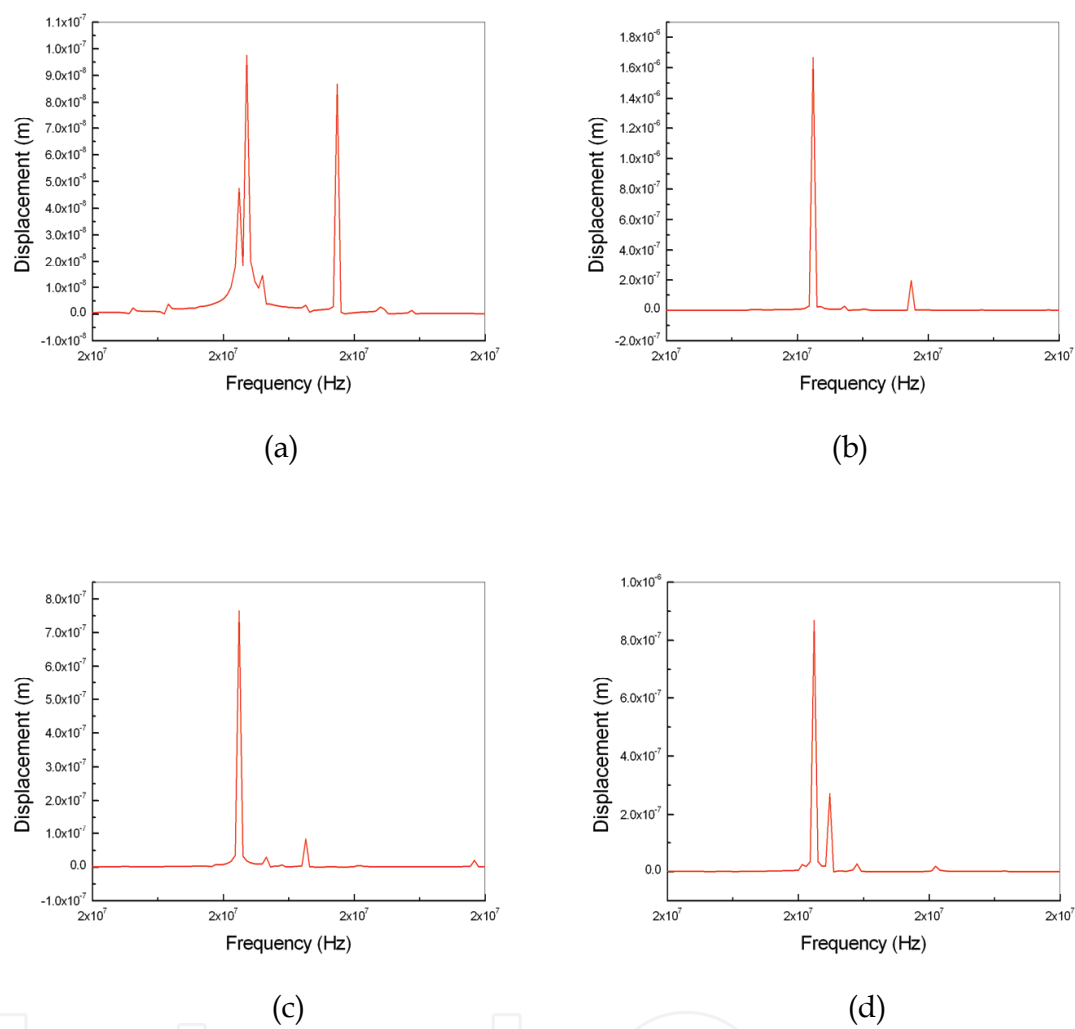


Figure 10. Frequency displacement of resonator using TE2 mode (a) electrode diameter = 0.3 mm; (b) electrode diameter = 0.4 mm; (c) electrode diameter = 0.5 mm; (d) electrode diameter = 0.6 mm

Fig. 11 shows the displacement distribution of the resonator when a TE2 mode vibration occurs. The rectangular part in this figure represents the area of the electrode. We can see that most displacements occurred concentratedly in the electrode.

4.3.3 Thickness Extensional Vibration (TE3 mode vibration)

This is because ceramic resonators that exhibit the energy trapping phenomenon of the TE3 mode vibration have better temperature characteristics and higher  $Q_m$  than those of the fundamental thickness vibration. However, resonators that use the TE3 mode vibration exhibit spurious responses of the TE1 mode vibration, the 5th-harmonic thickness extensional vibration etc.

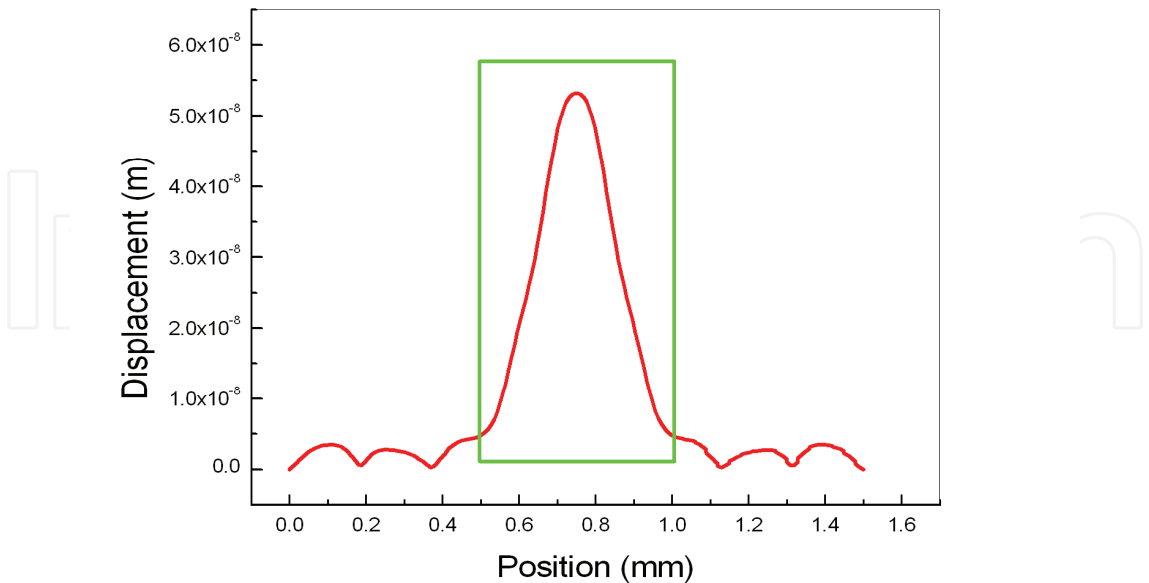


Figure 11. Distribution of inside displacement of resonator using TE2 mode vibration

There is the basic model of TE3 mode resonator in Fig. 12. It is 1.2 mm wide and 1.0 mm long. The height is set based on 0.068 mm. In case of the fixed point, boundary condition was set to have 0 displacement at the end of the resonator’s 4 exterior faces. Poling is in thickness direction. Round electrodes were attached to both top and bottom sides of resonator to supply the voltage here. Poling direction and voltage direction were set to be same in order to make the TE3 mode vibration occur. Fig. 13 and Fig. 14 show typical deformation and the displacement distribution of deformation. As shown in the figure, it is expected that other spurious vibration can affect more likely, because the displacement occurs at the whole resonator.

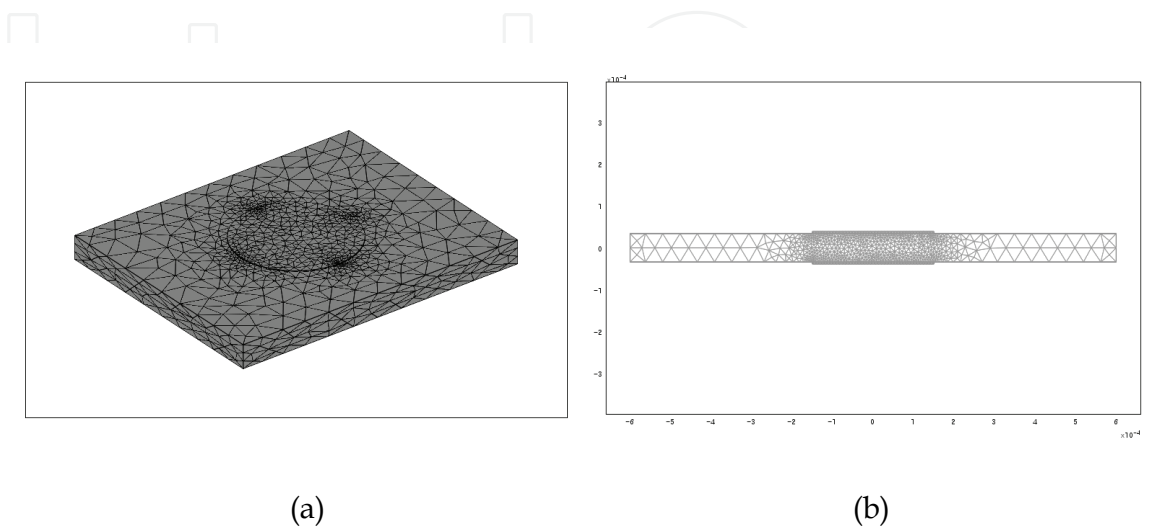


Figure 12. Simulation model for resonator using TE3 mode vibration

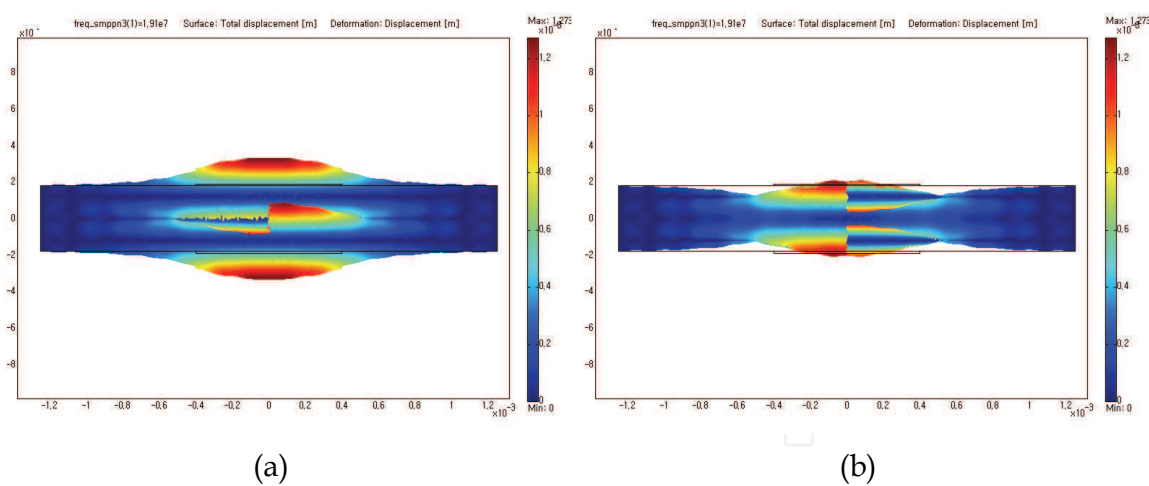


Figure 13. Vibration shape of TE3 mode vibration

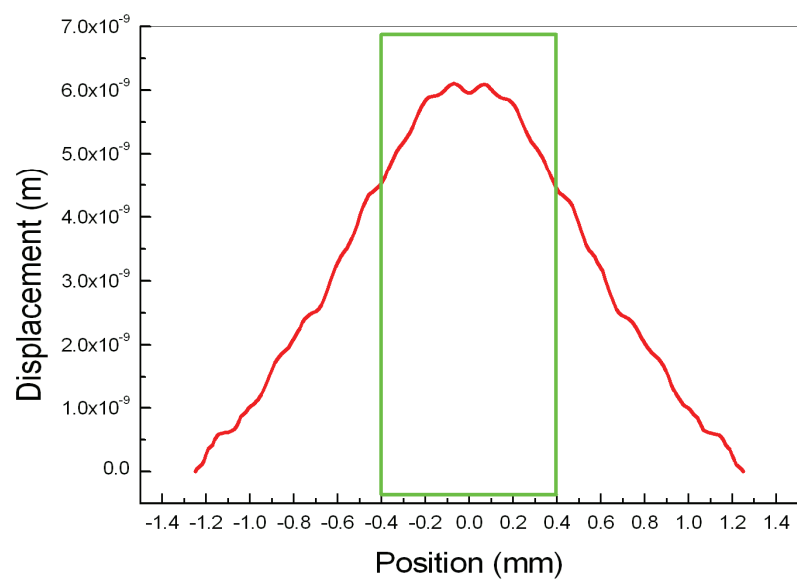


Figure 14. Distribution of inside displacement of resonator using TE3 mode vibration

TE3 mode resonator requires more precise control in manufacturing because it is more likely affected by spurious vibration compared to resonators using thickness shear vibration or TE2 vibration. The most influential variable on impedance waveform in TE3 mode resonator is of course the ratio of a electrode diameter and a resonator thickness. The influence of the ratio can be found by observing the influence of electrode diameter maintaining constant thickness of resonator. It is found that when electrode diameter becomes larger, the resonant frequency of a fundamental vibration and a spurious vibration become closer, and the amplitude of spurious vibration becomes also bigger. When the diameter of electrode is larger than 0.25 mm, the resonant frequency of spurious vibration and the anti-resonant frequency becomes very close to lead a break in the waveform of anti-resonant impedance of the fundamental vibration. Then anti-resonant impedance of the spurious vibration became higher than that of the fundamental vibration. On the other hand, when the diameter of electrode becomes less than 0.15, it was found that although the influence of the spurious

vibration occurring on high frequency becomes insignificant, other vibrations have influence near the resonant frequency. This reflects the possibility of the assumption that the spurious vibration of high frequency range moved close to the resonant frequency as the electrode diameter decreases, or the possibility of influence from other vibration. However, the certain cause has not been found yet. The thickness of the resonator is fixed to certain dimension corresponding to the frequency when the desired frequency is determined. Therefore, the optimal configuration can be designed by carefully controlling the ratio of the electrode diameter and the resonator thickness.

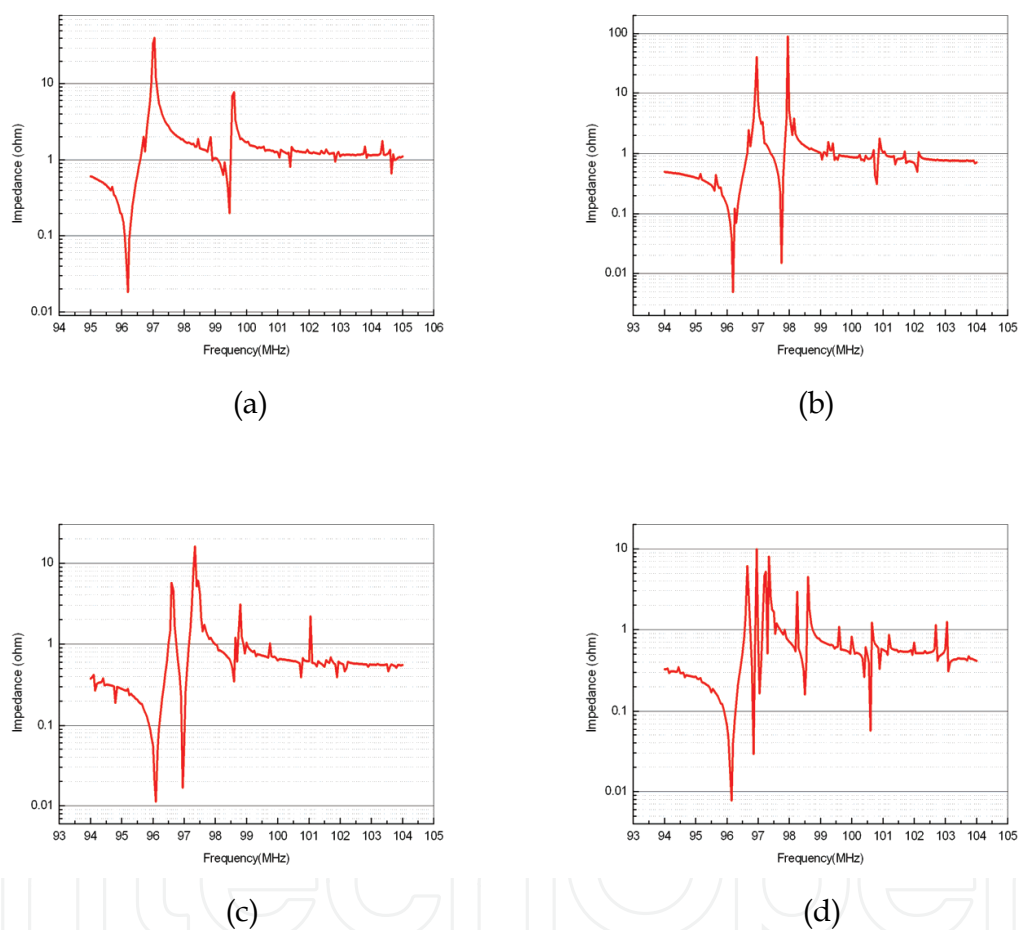


Figure 15. Impedance by the frequency of resonator using TE3 mode. (a) electrode diameter = 0.15 mm; (b) electrode diameter = 0.25 mm; (c) electrode diameter = 0.35 mm; (d) electrode diameter = 0.4 mm

In TE3 mode resonator, spurious vibration is always accompanied on slightly higher frequency along with the 3<sup>rd</sup> overtone vibration. Therefore, through the simulation study, we can find out the cause of spurious vibration and which variable affect on spurious vibration. Fig. 16 shows the form of the 3<sup>rd</sup> thickness vibration and of the following spurious vibration. Various examples of the influence of the strength and location of the spurious vibration on the impedance of 3<sup>rd</sup> vibration are shown. These are waveforms of impedance which is found in actual commercial products.



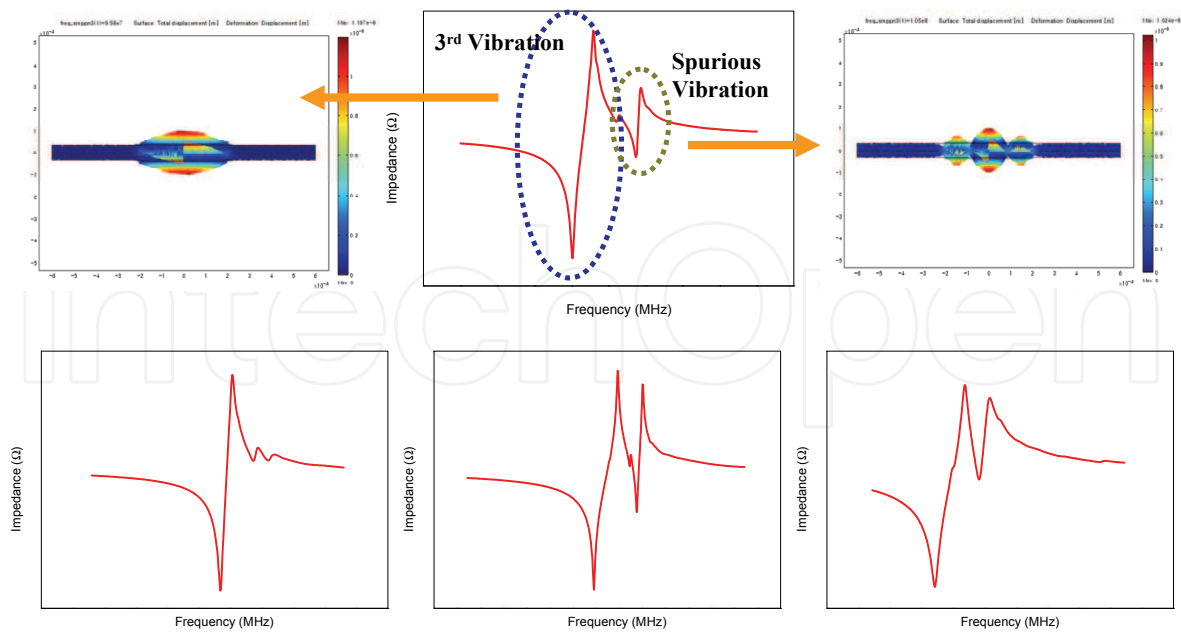


Figure 16. The effect of the interaction of TE3 mode vibration and spurious vibration on the impedance configuration

Therefore, the most important factor in designing a TE3 mode resonator shape is to make the spurious vibration, shown in the Fig. 16, occur as far as possible from the 3<sup>rd</sup> overtone vibration, or to design a shape that can minimize the amplitude.

Fig. 17(a) and (b) show the resonant frequency of the 3<sup>rd</sup> overtone vibration and the spurious vibration with the resonator thickness and the electrode diameter respectively. In case of the 3<sup>rd</sup> overtone vibration, the frequency constant was 1421, and the frequency constant of the spurious vibration was expected to be 1409. Also, we found out that while the resonant frequency of the 3<sup>rd</sup> vibration just slightly decreased as the diameter of electrode increased, the resonant frequency of the spurious vibration rapidly decreased. That is, we could expect that the 3<sup>rd</sup> vibration would be less influenced by the spurious vibration as the resonant frequency of the 3<sup>rd</sup> vibration and that of the spurious vibration become distant.

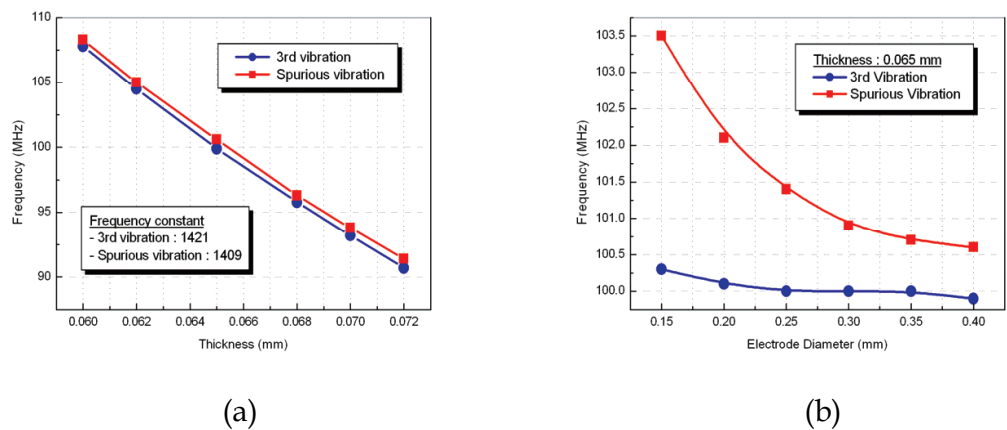


Figure 17. The effect of resonator thickness and electrode diameter on resonant frequency

## 5. Conclusion & Discussion

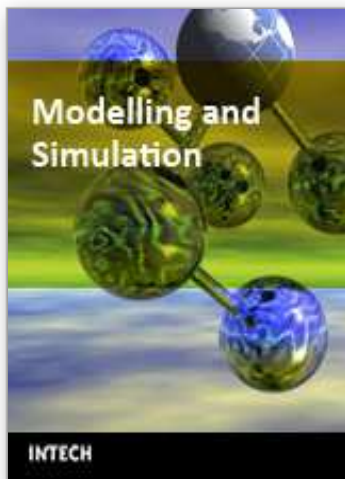
The ceramic manufacturing process is so complicated and process-dependent, that achieving reproducibility is very hard in many cases. Especially, ceramic resonator is smaller than other piezoelectric ceramics applications and more precise process control is needed. Therefore, understanding configuration design and tendency through simulation is very useful to avoid unnecessary effort. In recent trend, as piezoelectric ceramics is used in the various actuators and sensors, the use of simulation in this field is also increasing. Some of actuator, sensor or acoustic applications may have a complicated shape depending on the purposes, however, basic simulation process was regarded as same as resonator. Therefore, the accuracy of simulation depends on the accuracy of the knowledge on the material constants of piezoelectrics.

## 6. References

- A. Ando, T. Kittaka, T. Okada, Y. Sakabe and K. Wakino, Energy Trapping Characteristics of the Second Harmonic Thickness Extensional Vibration in a Two-Layered Monolithic Piezoelectric Plate, *Ferroelectrics*, Vol. 112, 1990, pp. 141-153.
- A. Ando, T. Sawada, H. Ogawa, M. Kimura and Y. Sakabe, Fine-Tolerance Resonator Application of Bismuth-Layer-Structured Ferroelectric Ceramics, *Jpn J. Appl. Phys.*, Vol. 41, (2002) 7057-7061.
- A. Ando, M. Kimura and Y. Kakabe, Piezoelectric Resonance Characteristics of  $\text{SrBi}_2\text{Nb}_2\text{O}_9$ -based Ceramics, *Jpn J. Appl. Phys.*, Vol. 42, (2003) 150-156.
- T. Azuma, J. Yamazaki, M. Inoue and K. Miyabe, Investigation of Spurious Mode in Piezoelectric Ceramic Resonators using Optical Fiber Interferometric Sensing, *Journal of the Korean Physical Society*, Vol. 32, February 1998, pp. S1294-S1297.
- S. E. Cummins and L. E. Cross, Electrical and Optical Properties of Ferroelectric  $\text{Bi}_4\text{Ti}_3\text{O}_{12}$  Single Crystals, *J. Appl. Phys.*, 39 (1968) 2268.
- H. Fan, L. Zhang, X. Yao, Relaxation Characteristics of Strontium Barium Niobate Ferroelectric Ceramics, *J. Mater. Sci.*, 33 (1998) 895-900.
- A. Fouskova and L. E. Cross, Dielectric Properties of Bismuth Titanate, *J. Appl. Phys.*, 41 (1970) 2834.
- C. Fujioka, R. Aoyagi, H. Takeda, S. Okamura and T. Shiosaki, Effect of non-stoichiometry on ferroelectricity and piezoelectricity in strontium bismuth tantalite ceramics, *Journal of the European Ceramic Society*, 25 (2005) 2723-2726.
- C. Galassi. (2000), *Piezoelectric Materials: Advances in Science, Technology and Applications*, pp. 14-17, Kluwer Academic Publishers, 0-7923-6212-8, Dordrecht.
- H. Kaida and J. Inoue, Strip-Type Resonators Using-Second-Harmonic Thickness-Extensional Vibration, *Jpn. J. Appl. Phys.*, Vol. 40, 2001, pp. 3680-3682.
- D. J. Kim, J. H. Lee and D. K. Kim. (2001). *An Introduction to the Mechanical Properties of Ceramics*, pp.48-49, Scitechmedia, Inc., 89-88397-78-9, Seoul. (Korean)
- M. Kimura, T. Sawada, A. Ando and U. Sakabe, Energy Trapping Characteristics of Bismuth Layer Structured Compound  $\text{CaBi}_4\text{Ti}_4\text{O}_{15}$ , *Jpn J. Appl. Phys.*, Vol. 38, (1999) 5557-5560.
- C. K. Lee, J. K. Moon and S. D. Lee, Dielectric Properties of ferroelectric  $\text{Sr}_{0.5}\text{Ba}_{0.5}\text{Nb}_2\text{O}_6$  cermaics, *J. Basic Sciences*, Vol.17 (2003) 45-52.

- D. J. Leo. (2007), *Smart Material Systems*, pp.122, John Wiley & Sons, Inc., 978-0-471-68477-0, Hoboken, New Jersey.
- T. Mitsui and S. Nomura. (1981). *Ferroelectrics and Related Substances*, Springer-Verlag, 0-387-09880-1, Berlin-Heidelberg.
- R. R. Neurgaonkar, W. F. Hall, J. R. Oliver, W. W. Ho and W. K. Copy, Tungsten Bronze  $\text{Sr}_{1-x}\text{Ba}_x\text{Nb}_2\text{O}_6$  – A Case History of Versatility, *Ferroelectrics*, Vol. 87, 1988, pp. 167-179.
- R. E. Newnham, R. W. Wolfe and J. F. Drrian, Structural Basis of Ferroelectricity in the Bismuth Titanate Family, *Mater. Res. Bull.*, 6, 1029 (1971).
- H. Ogawa, M. Kimura, A. Ando and Y. Sakabe, Temperature Dependence of Piezoelectric Properties of Grain-Oriented  $\text{CaBi}_4\text{Ti}_4\text{O}_{15}$  Ceramics, *Jpn J. Appl. Phys.*, Vol. 40, (2001) 5715-5718.
- G. A. Smolenskii, V. A. Bokov, V. A. Isupov, N. N. Krainik, R. E. Pasynkov, and A. I. Sokolov. (1984). *Ferroelectrics and Related Materials*, Gordon and Breach Science Publishers, 2-88124-107-7, New York.
- M. G. Stachiotti, C. O. Rodriguez, C. Ambrosch-Draxl and N. E. Christensen, Electronic structure and ferroelectricity in  $\text{SrBi}_2\text{Ta}_2\text{O}_9$ , *Phys. Rev. B*, 61 (2000) 14434-14439.
- E. C. Subbarao, A Family of Ferroelectric Bismuth Compounds, *J. Phys. Chem. Solid*, Vol. 23, (1962) 655.
- Y. Yamashita, S. Sakano, and Isamu Toba, TE Harmonic Overtone Mode Energy-Trapped Ceramic Filter with Narrow Frequency Tolerance, *Jpn J. Appl. Phys.*, Vol. 36, (1997) 6096-6102.

IntechOpen



## **Modelling and Simulation**

Edited by Giuseppe Petrone and Giuliano Cammarata

ISBN 978-3-902613-25-7

Hard cover, 688 pages

**Publisher** I-Tech Education and Publishing

**Published online** 01, June, 2008

**Published in print edition** June, 2008

This book collects original and innovative research studies concerning modeling and simulation of physical systems in a very wide range of applications, encompassing micro-electro-mechanical systems, measurement instrumentations, catalytic reactors, biomechanical applications, biological and chemical sensors, magnetosensitive materials, silicon photonic devices, electronic devices, optical fibers, electro-microfluidic systems, composite materials, fuel cells, indoor air-conditioning systems, active magnetic levitation systems and more. Some of the most recent numerical techniques, as well as some of the software among the most accurate and sophisticated in treating complex systems, are applied in order to exhaustively contribute in knowledge advances.

### **How to reference**

In order to correctly reference this scholarly work, feel free to copy and paste the following:

Jeong-Ho Cho, Yong-Hyun Lee, Myung-Pyo Chun and Byung-Ik Kim (2008). Practical Application of Simulation Technique for the Resonators Using Piezoelectric Ceramics, Modelling and Simulation, Giuseppe Petrone and Giuliano Cammarata (Ed.), ISBN: 978-3-902613-25-7, InTech, Available from:

[http://www.intechopen.com/books/modelling\\_and\\_simulation/practical\\_application\\_of\\_simulation\\_technique\\_for\\_the\\_resonators\\_using\\_piezoelectric\\_ceramics](http://www.intechopen.com/books/modelling_and_simulation/practical_application_of_simulation_technique_for_the_resonators_using_piezoelectric_ceramics)

**INTECH**  
open science | open minds

### **InTech Europe**

University Campus STeP Ri  
Slavka Krautzeka 83/A  
51000 Rijeka, Croatia  
Phone: +385 (51) 770 447  
Fax: +385 (51) 686 166  
[www.intechopen.com](http://www.intechopen.com)

### **InTech China**

Unit 405, Office Block, Hotel Equatorial Shanghai  
No.65, Yan An Road (West), Shanghai, 200040, China  
中国上海市延安西路65号上海国际贵都大饭店办公楼405单元  
Phone: +86-21-62489820  
Fax: +86-21-62489821

© 2008 The Author(s). Licensee IntechOpen. This chapter is distributed under the terms of the [Creative Commons Attribution-NonCommercial-ShareAlike-3.0 License](https://creativecommons.org/licenses/by-nc-sa/3.0/), which permits use, distribution and reproduction for non-commercial purposes, provided the original is properly cited and derivative works building on this content are distributed under the same license.

IntechOpen

IntechOpen